THE JOURNAL OF PHYSICAL CHEMISTRY C

Article

pubs.acs.org/JPCC

Sulfur/Carbon Nanotube Composite Film as a Flexible Cathode for Lithium−Sulfur Batteries

Kangke Jin, Xufeng Zhou,* Liangzhong Zhang, Xing Xin, Guohua Wang, and Zhaoping Liu*

Ningbo Institute of Material Technology and Engineering (NIMTE), Chinese Academy of Sciences, Ningbo 315201, P. R. China

Supporting Information

ABSTRACT: A flexible composite film composed of carbon nanotubes (CNTs) and sulfur as the cathode for lithium−sulfur (Li−S) batteries is prepared by coating an ultrathin sulfur nanolayer on a preprepared CNT film through a simple two-step heating process. The sulfur−CNT composite film with an areal density of ∼5 mg cm^{-2} has a high sulfur content of 65 wt % and is tough enough to be directly employed as the cathode in Li−S cells without binders, conductive additives, and current collectors. The porous and film-like CNT matrices enormously improve the electrical conductivity of sulfur and offer 3D pathways for fast Li ion diffusion, while the strong covalent bonds formed between sulfur and CNTs ensure the stability of sulfur during charge/discharge. Consequently, the film electrode delivers an initial capacity of 1100 mA h g^{-1} and can retain a reversible capacity of 740 mA h g^{-1} after 100 charge/discharge cycles at 0.1 C. It also shows good rate capability that a reversible capacity of 520 mA h g^{-1} can be reached at the rate of 2 C. Moreover, the high sulfur content gives rise to a high energy density of ∼1200 W h kg^{-1} based on the total mass of the electrode.

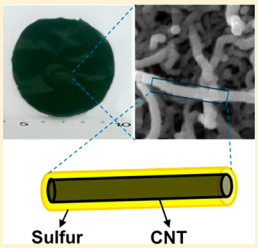

INTRODUCTION

Facing an increasing demand for green and renewable energy, it is urgently desirable to develop efficient energy storage systems with high energy density, long life, low cost, and environmental benignity.[1,2] The lithium−sulfur (Li−S) battery is one of the most promising candidates for energy storage devices. The sulfur cathode has a much higher theoretical capacity (1672 mA h g^{-1}) than conventional cathode materials currently used in lithium ion batteries, assuming complete reaction between Li and S.[3−5] Other advantages of sulfur include its extremely low cost, low equivalent weight, nontoxicity, and widespread availability. Consequently, it is anticipated that Li−S batteries will play important roles in the next-generation energy storage systems.[6,7] However, the electrochemical performance, especially the cycling stability of Li−S batteries at the current level, is not competent for practical applications, which is mainly due to the poor electrical conductivity (5×10^{-30} S cm^{-1}) of sulfur, the dissolution of polysulfide intermediates in electrolytes, and the relatively large volume variation of sulfur during charge/discharge processes.[8−12]

Modification of sulfur by carbonaceous materials with excellent electrical conductivity and low density has been proved effective to conquer the intrinsic deficiencies of sulfur.[13] To facilitate fast transport of electrons and Li ions, homogeneous and intimate contact between sulfur and carbon at the nanoscale needs to be realized by careful structural design. Fortunately, the diversity of carbonaceous materials provides scientists with opportunities to tune the architecture of the sulfur/carbon composites.[14−17] One successful example was reported by Ji et al. in 2009.[14] A sulfur−carbon interwoven nanostructure was constructed by filling sulfur in the tube-like nanopores of mesoporous carbon. The carbon network not only served as an excellent conducting agent but also trapped the polysulfides during redox. Therefore, a relatively high capacity up to 1320 mA h g^{-1} could be reached. However, the fully filled mesopores hindered the penetration of electrolytes, which was unfavorable to fast diffusion of Li ions and gave rise to limited rate capability.[18,19] Therefore, accessible pores within the sulfur/carbon composites are essential to shorten the diffusion length of Li ions. The carbon nanotube (CNT), which has an anisotropic 1D and flexible nanostructure, is suitable for the construction of nanoporous structures and has been extensively used in the modification of the sulfur cathode.[20−27]

The structure of the sulfur−CNT (S−CNT) composites significantly affects their electrochemical performance. In some recent studies, S−CNT composites with a structure of a thin layer of sulfur coated on the outer surface of CNTs were reported and exhibited enhanced electrochemical performance.[20,22] The intimate contact between sulfur and CNTs guaranteed fast electron transport within each composite nanotube, and sulfur was readily exposed to electrolytes, which was beneficial for the rapid diffusion of Li ions.

It needs to be noted that additional additives, including electrical conductive agents and binders, are usually required in fabricating the sulfur cathode for Li−S batteries. As a result, the proportion of sulfur in the final electrode is relatively low, which enormously reduces the energy density of the Li−S batteries. Consequently, it is important to increase the sulfur content in the electrode while still retaining its high utilization. Binder-free and film-like S−CNT electrodes prepared by chemical vapor deposition (CVD) were thus proposed recently.[28,29] Nevertheless, the CVD method is not cost-

Received: July 9, 2013
Revised: September 17, 2013
Published: September 19, 2013

   dx.doi.org/10.1021/jp406757w | J. Phys. Chem. C 2013, 117, 21112−21119

effective and requires harsh experimental conditions. Most recently, a self-weaving paper-like S-CNT composite cathode was reported by Su et al. through a relatively simple solution-based process.[30] An average energy density of 852 W h kg^{-1} based on the total mass of the cathode could be achieved. Unfortunately, a large amount of CNTs were utilized to guarantee the good electrochemical performance of the composite, which resulted in a relatively low sulfur content of 40 wt %. The energy density is expected to be further increased if the content of CNTs can be reduced. It should be pointed out that the interaction between sulfur and the conducting agents also plays an important role in the electrochemical performance of the sulfur cathode. In a recent paper reporting a sulfur/graphene composite cathode material, the formation of covalent bonds between oxygenic groups in graphene oxide and sulfur by thermal treatment was presented and considered to be essential to raise the charge/discharge stability of the composite.[31] It is noted that in Su's work the deposition of sulfur was conducted at room temperature, and pristine CNTs with no functional groups were employed. Such reaction conditions are not favorable for generating strong interactions between two components. If the formation of covalent bonds between sulfur and CNTs can be realized, the dissolution of sulfur is expected be further suppressed, which is beneficial for improving the cycling stability of the sulfur cathode.

In this paper, a simple method to prepare flexible and porous S−CNT composite film which can be directly used as the cathode for Li−S batteries is proposed. Using slightly oxidized CNT film preprepared by vacuum filtration[32,33] as a conductive and flexible framework, thin sulfur layers having a thickness of ∼10 nm can be homogeneously coated onto the surface of each CNT. Since oxygenic groups are generated on the surface of preoxidized CNTs and a two-step heating process was involved in the experiments, the formation of strong covalent bonds between sulfur and CNTs is successfully realized. Together with the high electrical conductivity of the CNT network, the thin thickness of the sulfur layer, and the open nanopores within the film, the S−CNT composite film exhibits outstanding electrochemical performance. Moreover, the high sulfur content of 65 wt % results in high energy density of ∼1200 W h kg^{-1} based on the total mass of the electrode.

EXPERIMENTAL SECTION

Preparation of CNT Film. The raw multiwalled CNTs (∼20 nm in diameter, purchased from Shenzhen Nanotech Port Co. Ltd., China) were first refluxed in the concentrated H_2SO_4/HNO_3 (3:1, v:v) solution at 80 °C for 0.5 h and then washed with distilled water until the pH value reached 7. Then the oxidized CNTs were dispersed in distilled water with rapid stirring for 2 h. The CNT film was finally obtained by filtrating the above dispersion through a porous polytetraflouroethylene membrane and drying in air.

Preparation of S−CNT Film. Typically, 5 g of sulfur was put into a crucible and heated in an oven at the temperature of 155 °C. After the sulfur was completely melted, a CNT film prepared in the first step was immersed in the sulfur melt and heated at 155 °C for 12 h. Then, the film was taken out and transferred to another clean crucible and heated under vacuum for another 6 h. Excessive sulfur filled in the nanopores of the CNT film was drained and evaporated during this heating process. After cooling to room temperature, a small amount of sulfur sticking to the bottom surface of the film was wiped using ethanol, and then the S−CNT film was finally obtained.

Preparation of S−CNT Composite Powder. In a typical preparation process, 0.65 g of sulfur and 0.35 g of oxidized CNTs were mechanically mixed by high-energy ball milling for 2 h. Then the mixture was transferred into an oven and kept at the temperature of 155 °C for 18 h. After cooling to room temperature, the S−CNT composite powder was obtained.

Material Characterizations. Electron microscopic images were recorded by a Hitachi S-4800 field emission scanning electron microscope (SEM) and an FEI Tecnai G2 F20 transmission electron microscopy (TEM) at an accelerating voltage of 200 kV. Thermogravimetric analysis (TGA) was performed on a TGA50 analyzer (Shimadzu) under N_2 atmosphere. X-ray photoelectron spectra (XPS) were recorded by an AXIS ULTAR^{DLD} spectroscope from Kratos. Raman spectroscopy was collected with 532 nm laser under ambient conditions with a JY HR800 spectrometer (Renishaw), and the laser spot size is ∼1 μm. The Brunauer−Emmett−Teller (BET) surface area and the pore volume were measured using a QuadraSorb surface area analyzer.

Electrochemical Measurement. The S−CNT film was used as the cathode directly, and the total material loading density was ∼5 mg cm^{-2}. For the S−CNT composite powder, it was first mixed with Super P and polyvinyldifluoride (Kynar HSV 900), with a mass ratio of 80:10:10, in *N*-methylpyrrolidone to produce electrode slurry. The slurry was then casted onto an aluminum foil current collector and dried at 80 °C for 12 h to form the cathode. The total material loading density was ∼3 mg cm^{-2}.

Two cathodes described above were then assembled into 2032-type coin cells inside an Ar-filled glovebox using Li metal foil as the anode, 1.0 M lithium bistrifluoromethane sulfonylimide in 1,3-dioxolane and 1,2-dimethoxyethane (volume ratio 1:1) as the electrolyte, and 0.1 wt % $LiNO_3$ as the additive.[34] A LAND-CT2001A battery test system (Jinnuo Wuhan Corp., China) was used to perform the measurements. The current density varied from 0.1 to 2 C (1 C equals to 1672 mA g^{-1}). The charge−discharge voltage range was 1−3 V.

RESULTS AND DISCUSSION

The preparation route of the S−CNT composite film is illustrated in Figure 1. In the first step, CNTs were partially oxidized by refluxing in concentrated H_2SO_4/HNO_3 (3:1, v:v)

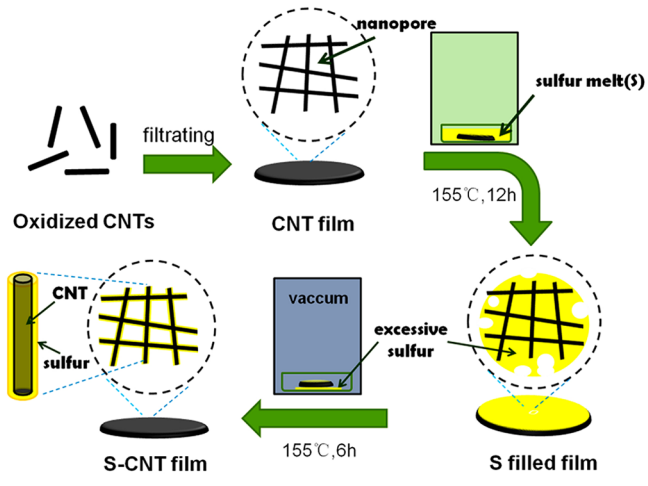

Figure 1. Illustration of the synthesis process for a S−CNT film and its structure model.

dx.doi.org/10.1021/jp406757w | J. Phys. Chem. C 2013, 117, 21112−21119

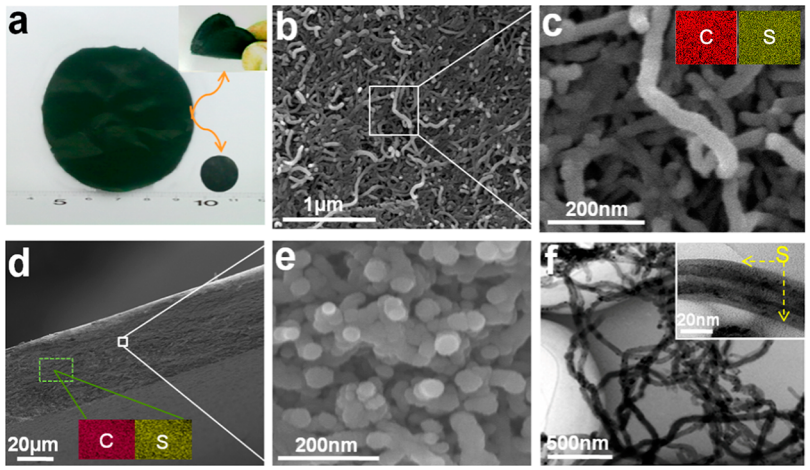

Figure 2. (a) Digital photograph of a flexible S−CNT film. Inset shows the film bent by hand. (b) SEM image of the front side of the S−CNT film at a low magnification. (c) SEM image of the front side of the S−CNT film at a high magnification and the corresponding C and S elemental mapping images. (d) SEM image of the cross section of the S−CNT film and the corresponding C and S elemental mapping images. (e) Magnified SEM image of the cross section of the S−CNT film. (f) TEM images of the S−CNT composite. Inset is a high-resolution image of an individual composite nanotube.

and then filtrated to form a continuous film with a porous structure (Figure S1, Supporting Information, for details). The surface modification of CNTs by oxidation can remarkably improve the dispersion of CNTs in solvents,[22] which is essential to form a uniform film. In addition, the oxygenic groups on the surface can enhance the interaction between CNTs and sulfur.[31] The CNT film was then immersed in sulfur melt which had been preheated to 155 °C and kept at the same temperature for 12 h. During this process, the sulfur melt was gradually sucked into and finally fully filled the pores in the CNT film. It should be mentioned that sulfur melt has the lowest surface tension at 155 °C.[18,19] Therefore, this temperature was chosen as the heating temperature in our experiments to benefit the impregnation of sulfur melt. Afterward, the composite film was removed from the sulfur melt and heated at 155 °C for another 6 h in vacuum to drain and evaporate excessive sulfur which blocked the pores. After cooling to room temperature, a porous composite film composed of CNTs and sulfur as the cathode for the Li−S battery was finally obtained. Using TGA, the content of sulfur in the composite film is estimated to be ∼65 wt % (Figure S2, Supporting Information).

As shown in Figure 2a, the S−CNT composite film having an area of ∼10 cm^2 and an areal density of ∼5 mg cm^{-2} is flexible, which can be bent back and forth continuously without generating fractures (inset of Figure 2a). The film also shows good toughness. It stays unbroken after it was punched with small round pieces of ∼1 cm in diameter for electrochemical measurement (lower right of Figure 2a). The front-side view of the S−CNT film under SEM is displayed in Figure 2b and 2c. A low-magnification SEM image (Figure 2b) shows that the composite film has a relatively smooth surface, and no large particles or aggregates are observed. In an SEM image with a higher magnification (Figure 2c), it is found that the composite film is composed of intertwined nanotubes. The average diameter of the nanotubes is measured to be ∼40 nm, which is approximately twice that of the pristine CNTs (Figure S1, Supporting Information), indicating a uniform coating of sulfur onto the surface of CNTs, and the thickness of the coating is calculated to be ∼10 nm. The surface of individual nanotubes becomes coarser compared with that of pure CNTs, which also implies successful loading of sulfur on the surface. The distribution of S in the sample is also characterized by elemental mapping. Though the resolution of the mapping is not high enough to identify individual CNTs with S coating layers, the uniform distribution of both C and S within the whole area indicates that S is homogeneously distributed in the CNT framework. Nanopores with width of tens of nanometers are clearly visible in the composite film, which is generated by random intertwining of nanotubes. The cross-section view of the S−CNT film under SEM as shown in Figure 2d indicates a uniform thickness of ∼40 μm of the film. The elemental mapping also reveals homogeneous distribution of sulfur over the entire film. Compared with the morphology of the S−CNT film on the surface (Figure 2c), similar porous structures constructed by nanotubes are also discerned within the interior of the composite film as shown in a further magnified SEM image of the film cross-section (Figure 2e), suggesting sufficient homogeneity of the as-prepared composite film using the two-step heating process. A large quantity of the nanotube terminals observed in the cross-section view imply that nanotubes tend to lie horizontally in the film. TEM characterization was then carried out to investigate the detailed structures of individual composite nanotubes. Samples were prepared by ultrasonic treatment of the composite film in ethanol, which untied the intertwined nanotubes. As shown in Figure 2f, the nanotubes have uniform diameters of ∼40 nm, which is coincident with the SEM results. The highly magnified TEM image of an individual nanotube is shown in the inset of Figure 2f. Comparing with the TEM image of pure CNTs (Figure S1c, Supporting Information), a thin layer as marked by yellow arrows in Figure 2f with a mean thickness of ∼10 nm wrapping on the outer surface of CNTs is discernible for the composite nanotube, which can be identified as sulfur deposited on CNTs. No isolated sulfur particles are detected in this sample, indicating that the interaction between sulfur and CNTs is strong enough to endure the harsh ultrasonic treatment. Nitrogen sorption measurement reveals that the S−CNT composite film has a relatively high BET surface area of 35.1 m^2 g^{-1} and a total pore volume of 0.25 cm^3 g^{-1}, which further verifies the existence of large amounts of nanopores within the composite film (Figure S3, Supporting Information). Such open nanopores are of great importance for mass transport,

dx.doi.org/10.1021/jp406757w | J. Phys. Chem. C 2013, 117, 21112−21119

thus are expected to be beneficial for the electrochemical performance of the S−CNT film. It should be pointed out that the second heating process in vacuum to drain and evaporate excessive sulfur is essential to the formation of the porous structure. Without such a heating procedure, the pores of the CNT film are almost fully filled with sulfur as reflected by the SEM images of the intermediate composite (Figure S4, Supporting Information). Such a dense structure gives rise to a small BET surface area of 6.69 $m^2 g^{-1}$ and a total pore volume of 0.04 $cm^3 g^{-1}$, both of which are approximately 1/6 of the corresponding values of the final product. Moreover, the large content of sulfur in the intermediate composite enormously reduces its strength and flexibility. The film crushes severely under mechanical impact, which makes it difficult to be manufactured into small pieces for electrochemical tests.

Figure 3a shows the XPS of the S−CNT film as well as pure sulfur for comparison. Two peaks centered at 227.0 and 162.9 eV are clearly found in the spectrum of the S−CNT film, which can be ascribed to the 1s and $2p^{3/2}$ signals of element sulfur, respectively. Both peaks shift to lower binding energy for ∼1 eV compared with their counterparts in the spectrum of pure sulfur, which can be attributed to the formation of covalent bonds directly between S and C or through the O bridge.[31] The interaction between sulfur and carbon is also verified by Raman characterization (Figure 3b). The peak centered at 485.5 cm^{-1} is characteristic of a S−S stretching vibration, while the one at 742.1 cm^{-1} indicates the formation of C−S bonds as reported before.[35] The covalent bonds between C and S are crucial to the formation of ultrathin S layers on CNTs. When most of the sulfur existing in the pores of CNT film was drained or evaporated at elevated temperatures, sulfur in intimate contact with CNTs can be grasped by the nanotubes through covalent bonds and finally remained as S shells covering the surface of CNTs. Such a strong interaction between sulfur and CNTs also guarantees the structural stability of the composite film during charge/discharge processes. It should be mentioned that preoxidation of CNTs in the HNO_3/H_2SO_4 mixture is critical to strongly anchor sulfur on their surface, as oxygenic groups are much more active than inert conjugated carbon atoms to bind sulfur.[31]

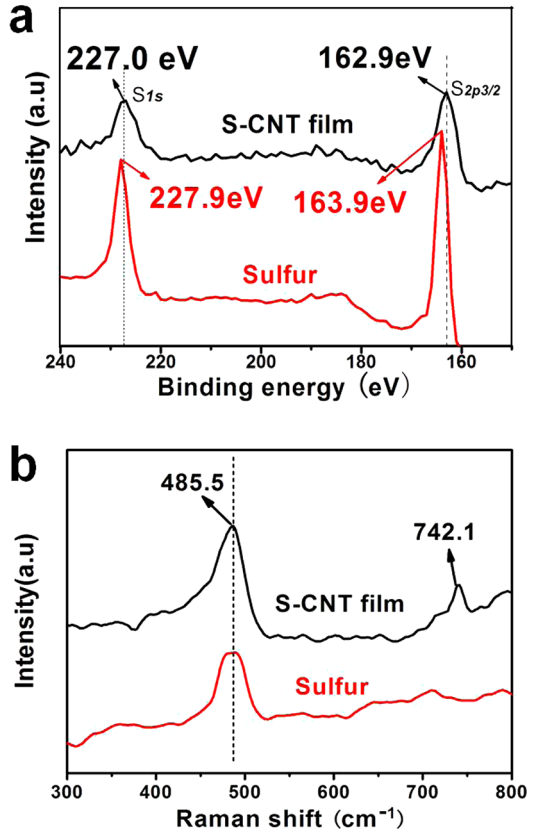

Figure 3. (a) XPS spectra of the S−CNT film and pure sulfur. (b) Raman spectra of the S−CNT film and pure sulfur.

To measure the electrochemical performance of the S−CNT composite film, the film was cut into round pieces of ∼1 cm in diameter and then directly used as the cathode with no current collectors. For comparison, powdery S−CNT composites were prepared by ball milling of sulfur and CNTs with the same mass ratio as that for the S−CNT film and following heating of the mixture at 155 °C to enhance the interaction between two components. SEM characterization (Figure S5, Supporting Information) shows that the homogeneous distribution of two components in the S−CNT composite powder is difficult to achieve even using high-energy ball milling. The size of S particles in the composite varies in a wide range, and the existence of large sulfur particles at the micrometer scale is inevitable. Conductive additives (carbon black), binders, and current collectors are needed to fabricate the electrode using the S−CNT composite powder as the active material, which results in a much lower weight content of sulfur (25 wt %) within the entire electrode compared with that in the case of the S−CNT film (65 wt %, see Table S1, Supporting Information, for details).

Figure 4 shows the cyclic voltammetry (CV) profiles of S−CNT film and S−CNT composite powder measured at a scan rate of 0.1 mV s^{-1} in the potential range of 1.0−3.0 V (vs Li/Li^+). An oxidation peak centered at ∼2.3 V and two reduction peaks at 2.0 and 2.3 V are observed for both samples, which are a characteristic CV response of the S anode. Though two samples have almost identical shape of the CV curves, it is obvious that the current densities of both oxidation and reduction peaks for the S−CNT film are higher than those of the S−CNT composite powder, indicating that the S−CNT film is able to deliver a higher capacity than the latter one.

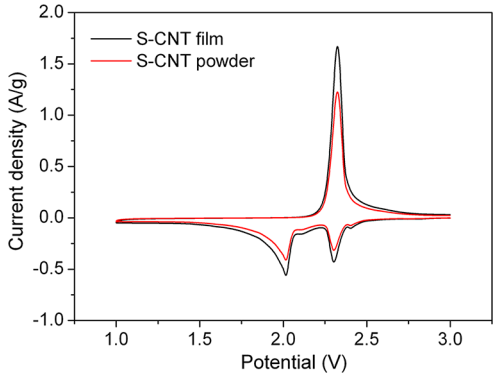

Figure 4. CV curves of S−CNT film and S−CNT composite powder at a scan rate of 0.1 mV s^{-1}.

The galvanostatic discharge/charge profiles at a 0.1 C rate of two cells using S−CNT film and S−CNT composite powder, respectively, as the cathode material are shown in Figure 5a. The film electrode has a discharge capacity of 1109 mA h g^{-1}

dx.doi.org/10.1021/jp406757w | J. Phys. Chem. C 2013, 117, 21112−21119

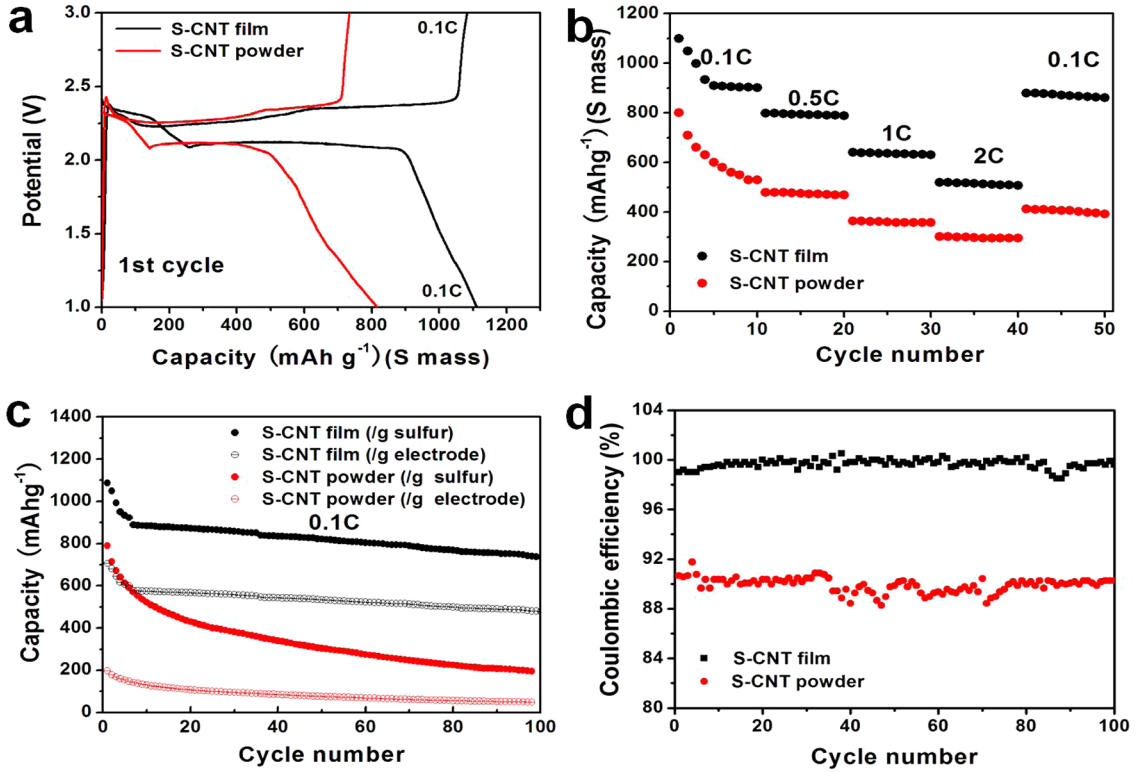

Figure 5. (a) Galvanostatic discharge/charge profiles of S−CNT film and S−CNT composite powder at a 0.1 C rate. (b) Reversible capacity of S−CNT film and S−CNT composite powder at varying charge/discharge rates. (c) Cycling profiles of S−CNT film and S−CNT composite powder at a constant current rate of 0.1 C. (d) Coulombic efficiencies of S−CNT film and S−CNT composite powder during 100 charge/discharge cycles.

and a charge capacity of 1097 mA h g^{-1} (related to the sulfur mass) within the first cycle, representing a very high sulfur utilization. The corresponding Coulombic efficiency in the first cycle is 98.9%. For comparison, the powdery S−CNT cathode material only has a discharge capacity of 813 mA h g^{-1}, a charge capacity of 733 mAh g^{-1}, and the Coulombic efficiency of 90.1%, all much lower than those of the S−CNT film, which is in good accordance with the CV data. The existence of relatively large insulating sulfur particles in the S−CNT composite powder, which is unfavorable to the diffusion of both Li^+ and electrons, is believed to cause the low utilization of active sulfur materials. Electrochemical impedance spectroscopy measurement (Figure S6, Supporting Information) reveals that the charge-transfer resistance of the S−CNT film is apparently smaller than that of the S−CNT composite powder, which verifies the advantage of the film-like CNT network in improving the electrical conductivity of sulfur over the powdery mixture.

The rate capability of the S−CNT film and S−CNT composite powder was then evaluated by cycling the cells at elevated charge/discharge rates up to 2 C. The reversible capacities at varying rates are plotted in Figure 5b, and typical galvanostatic charge−discharge curves at different rates are shown in Figure S7 (Supporting Information). For the S−CNT film, an average capacity decay of ∼60 mA h g^{-1} per cycle is observed during the first four charge/discharge cycles at 0.1 C. After the fifth cycle, the cell reaches a steady reversible capacity of ∼900 mA h g^{-1}. A capacity of 798 mA h g^{-1} can be delivered at a higher rate of 0.5 C. Further increasing the charge/discharge rate to 1 and 2 C, a reversible capacity of 641 mA h g^{-1} (58% of its initial capacity) and 520 mA h g^{-1} (47% of its initial capacity) is reached, respectively. The cell also demonstrates excellent stability at each rate between 0.5 and 2 C. When the charge/discharge rate is back to 0.1 C after being cycled at high rates for 30 times, a reversible capacity of ∼900 mA h g^{-1}, which equals the ones reached during the initial 5th to 10th cycles at 0.1 C, can be restored, suggesting excellent redox stability of the S−CNT film. Compared with the S−CNT film, the reversible capacity of the S−CNT composite powder decays continuously from ∼800 to ∼530 mA h g^{-1} during charge/discharge cycles at 0.1 C. Its reversible capacity at 0.5, 1, and 2 C rates is 480, 360, and 300 mA h g^{-1}, respectively, which is 60%, 56%, and 57% of the corresponding capacity for S−CNT film, respectively. The capacity of ∼400 mA h g^{-1} was obtained when the cell was remeasured at 0.1 C after high rate tests, which is even lower than the values measured at 0.5 C. Consequently, S−CNT film displays remarkably better rate capability than S−CNT composite powder. The cycling stability of both cathode materials was then evaluated by charge/discharge cycling of the cells at a rate of 0.1 C for 100 times, and the results are shown in Figure 4c. Similar to its rate performance displayed in Figure 5b, a relatively fast decay of the discharge capacity of the S−CNT film occurs during the initial several cycles. After a total capacity loss of ∼200 mA h g^{-1} (18% of the initial capacity) at the end of the seventh cycle, the decay rate of the cell dramatically decreases until the 100th cycle. The cell can still deliver a capacity of 740 mA h g^{-1} (67% of the initial capacity) after 100 cycles. The decay rate per cycle during the 7th−100th cycles is as small as 0.19%, reflecting excellent cycling stability of the S−CNT film. The relatively large capacity loss during the first several cycles is supposed to be caused by the outflow of sulfur on the outermost surface of the composite nanotubes, or some sulfur nanoparticle residues remain in the nanopores of the

dx.doi.org/10.1021/jp406757w | J. Phys. Chem. C 2013, 117, 21112−21119

film, both of which do not have a strong interaction with CNTs. However, the outstanding stability of the cell within the following 93 cycles suggests that the majority of the sulfur anchors firmly to the CNT network because of the strong chemical bonds formed between sulfur and the oxidized CNTs, as well as the ultrathin thickness of sulfur. On the contrary, the S−CNT composite powder shows much worse cycling stability. A continuous decrease of the discharge capacity from 800 mA h g^{-1} at the first cycle to 200 mA h g^{-1} at the 100th cycle is observed, which corresponds to a very low capacity retention rate of 25%. Different from the S−CNT film in which sulfur and CNTs have uniform and intimate contact at the nanoscale, the two components in the S−CNT composite powder are only mechanically mixed, which has an inevitable defect in homogeneity and lacks an efficient contact between sulfur and CNTs. Therefore, the S−CNT composite powder has a poor performance in cycling stability.

Another advantage of the S−CNT film over the composite powder is that the film can be directly used as the electrode without conductive additives, binders, and current collectors, which gives rise to a high content of active sulfur materials in the electrode and is beneficial for improving the energy density of the cells. The cycling profiles based on the total weight of the electrode are also displayed in Figure 5c. The weight content of sulfur reaches ∼65% for the S−CNT film electrode, while the corresponding value in the electrode using the S−CNT composite powder as the active material is as low as 25%. Consequently, an enormous capacity gap between two electrode materials based on the total mass of the electrode is observed. The initial discharge capacity of the S−CNT film (∼700 mA h g^{-1}) is ∼3.5 times higher than that of the S−CNT composite powder (∼200 mA h g^{-1}), and the ratio further increases to ∼10 (480 vs 50 mA h g^{-1}) after 100 time cycles. The average energy density based on the total mass of the S−CNT film within 100 cycles is calculated to be ∼1200 W h kg^{-1}, which is several times higher than that of conventional Li ion batteries.

The Coulombic efficiencies of the two cells with the charge/discharge cycles are depicted in Figure 5d. For the S−CNT film electrode, nearly 100% Coulombic efficiency can be achieved at each cycle, suggesting an excellent reversibility of the composite film during redox. The Coulombic efficiency for the composite powder, however, remains around 90% during all 100 cycles, which implies a relatively large outflow of sulfur during charge/discharge processes.

The S−CNT film electrode keeps intact, and no fracture occurs after long-time charge/discharge cycles, revealing good toughness of the composite film. The SEM image of the S−CNT film after 100 cycles (Figure 6a) clarifies that the diameters of the nanotubes remain almost the same as the ones before charge/discharge, suggesting sulfur wrapping on the surface of CNTs are stable during redox. The energy-dispersive spectrum (EDS) also indicates that there are remaining large quantities of sulfur after 100 cycles. TGA results (Figure 6b) further confirm that the sulfur content in the as-cycled film reaches 60 wt %. Assuming that the mass of CNTs keeps constant during cycling, it can be calculated that only ∼20% of sulfur detached from the electrode after 100 cycles. Consequently, the majority of sulfur can be successfully immobilized in the film-like cathode during charge/discharge processes, which is mainly attributed to the strong chemical bonds formed between sulfur and CNTs.

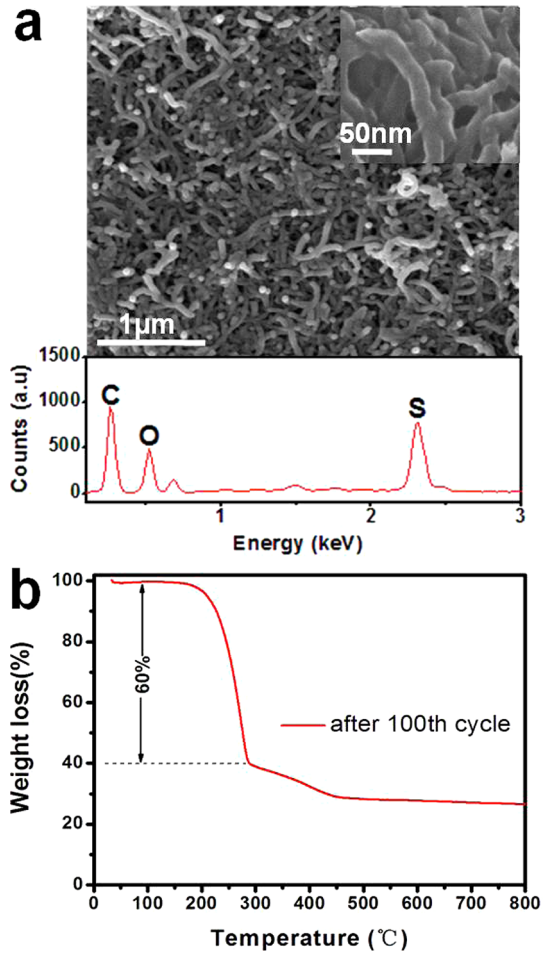

Figure 6. (a) SEM image of the S−CNT film after 100 cycles (above) and the EDS result of the film (below). (b) TGA curve of the S−CNT film after 100 cycles.

The excellent electrochemical performance of the S−CNT film can be ascribed to its unique structure. The randomly intertwined CNTs in the composite film construct a highly conductive network that facilitates fast transport of electrons within the entire film, while the ultrathin sulfur layer with a thickness of ∼10 nm on the CNTs enormously shortens the diffusion length of Li ions. Moreover, the porous structure of the S−CNT film enables easy infiltration of the electrolytes into the film and guarantees thorough exposure of sulfur-coating layers to Li ions in the electrolytes. Therefore, good rate capability can be achieved for the S−CNT film. On the other hand, the covalent bonds between two components in the composite film adhere sulfur layers strongly to the CNT matrices. As a result, sulfur and polysulfide intermediates can be immobilized within the S−CNT film during the electrochemical redox reactions, giving rise to superior cycling stability. In addition, the integration of conductive CNTs and sulfur into a film-like entity with a flexible feature generates notable advantages over conventional powdery S−CNT composites in terms of energy density, since no additional conductive additives, binders, and current collectors are needed during the fabrication of electrodes.

■ CONCLUSIONS

Flexible S−CNT composite film, prepared by casting ultrathin sulfur layers on the film-like CNT matrices, exhibits out-

dx.doi.org/10.1021/jp406757w | J. Phys. Chem. C 2013, 117, 21112−21119

standing rate capability and cycling stability as the cathode for Li−S batteries. An initial capacity of 1100 mA h g^{-1} and a retention rate of 67% after 100 charge/discharge cycles at 0.1 C can be achieved. Such S−CNT film can be directly used as the cathode without conductive additives, binders, and current collectors. Therefore, a reversible capacity higher than 600 mA h g^{-1}, corresponding to an energy density of ∼1200 W h kg^{-1}, is able to be reached based on the total mass of the electrode, which is notably higher than conventional powdery sulfur cathodes. Moreover, the preparation method of S−CNT film is relatively simple and cost-effective, which is expected to be practically applicable for high-performance Li−S batteries as the next-generation energy storage systems.

■ ASSOCIATED CONTENT

Supporting Information

Extended SEM and TEM images, Raman spectra, TGA curves, N_2 sorption characterization results, and data table. This material is available free of charge via the Internet at http://pubs.acs.org.

■ AUTHOR INFORMATION

Corresponding Authors

*E-mail: liuzp@nimte.ac.cn. Tel./Fax: +86-574-8668-5096.
*E-mail: zhouxf@nimte.ac.cn

Notes

The authors declare no competing financial interest.

■ ACKNOWLEDGMENTS

We are grateful for financial support from the Key Research Program of the Chinese Academy of Sciences (Grant No. KGZD-EW-202-4), Zhejiang Provincial Natural Science Foundation of China (Grant No. R4100194), Science and Technology Innovation Team of Ningbo (Grant No. 2012B82001), and the 973 Program (Grant No. 2011CB935900).

■ REFERENCES

(1) Armand, M.; Tarascon, J. M. Building Better Batteries. *Nature* **2008**, *451*, 652−657.
(2) Goodenough, J. B.; Kim, Y. Challenges for Rechargeable Li Batteries. *Chem. Mater.* **2010**, *22*, 587−603.
(3) Demir-Cakan, R.; Morcrette, M.; Nouar, F.; Davoisne, C.; Devic, T.; Gonbeau, D.; Dominko, R.; Serre, C.; Férey, G.; Tarascon, J.-M. Cathode Composites for Li−S Batteries via the Use of Oxygenated Porous Architectures. *J. Am. Chem. Soc.* **2011**, *133*, 16154−16160.
(4) Evers, S.; Nazar, L. F. Graphene-Enveloped Sulfur in a One Pot Reaction: a Cathode with Good Coulombic Efficiency and High Practical Sulfur Content. *Chem. Commun.* **2012**, *48*, 1233−1235.
(5) Lai, C.; Gao, X. P.; Zhang, B.; Yan, T. Y.; Zhou, Z. Synthesis and Electrochemical Performance of Sulfur/Highly Porous Carbon Composites. *J. Phys. Chem. C* **2009**, *113*, 4712−4716.
(6) Ryu, H. S.; Ahn, H. J.; Kim, K. W.; Ahn, J. H.; Lee, J. Y. Discharge Process of Li/PVDF/S Cells at Room Temperature. *J. Power Sources* **2006**, *153*, 360−364.
(7) Wang, J. L.; Yang, J.; Xie, J. Y.; Xu, N. X. A Novel Conductive Polymer−Sulfur Composite Cathode Material for Rechargeable Lithium Batteries. *Adv. Mater.* **2002**, *14*, 963−965.
(8) Ji, X. L.; Evers, S.; Black, R.; Nazar, L. F. Stabilizing Lithium−Sulfur Cathodes Using Polysulfide Reservoirs. *Nat. Commun.* **2011**, *2*, 325−31.
(9) Wang, J. Z.; Lu, L.; Choucair, M.; Stride, J. A.; Xu, X.; Liu, H. K. Sulfur-Graphene Composite for Rechargeable Lithium Batteries. *J. Power Sources* **2011**, *196*, 7030−7034.
(10) He, G.; Ji, X. L.; Nazar, L. F. High "C" Rate Li-S Cathodes: Sulfur Imbibed Bimodal Porous Carbons. *Energy Environ. Sci.* **2011**, *4*, 2878−2883.
(11) Cao, Y. L.; Li, X. L.; Aksay, I. A.; Lemmon, J.; Nie, Z. M.; Yang, Z. G.; Liu, J. Sandwich-type Functionalized Graphene Sheet-Sulfur Nanocomposite for Rechargeable Lithium Batteries. *Phys. Chem. Chem. Phys.* **2011**, *13*, 7660−7665.
(12) Jayaprakash, N.; Shen, J.; Moganty, S. S.; Corona, A.; Archer, L. A. Porous Hollow Carbon @ Sulfur Composites for High-Power Lithium-Sulfur Batteries. *Angew. Chem., Int. Ed.* **2011**, *50*, 5904−5908.
(13) Ji, X. L.; Nazar, L. F. Advances in Li−S Batteries. *J. Mater. Chem.* **2010**, *20*, 9821−9826.
(14) Ji, X. L.; Lee, K. T.; Nazar, L. F. A Highly Ordered Nanostructured Carbon−sulfur Cathode for Lithium−Sulfur Batteries. *Nat. Mater.* **2009**, *8*, 500−506.
(15) Wang, H. L.; Yang, Y.; Liang, Y. Y.; Robinson, J. T.; Li, Y. G.; Jackson, A.; Cui, Y.; Dai, H. J. Graphene-Wrapped Sulfur Particles as a Rechargeable Lithium Sulfur Battery Cathode Material with High Capacity and Cycling Stability. *Nano Lett.* **2011**, *11*, 2644−2647.
(16) Zheng, G. Y.; Yang, Y.; Cha, J. J.; Hong, S. S.; Cui, Y. Hollow Carbon Nanofiber-encapsulated Sulfur Cathodes for High Specific Capacity Rechargeable Lithium Batteries. *Nano Lett.* **2011**, *11*, 4462−4467.
(17) Li, N. W.; Zhang, M. B.; Lu, H. L.; Hu, Z. B.; Shen, C. F.; Chang, X. F.; Ji, G. B.; Cao, J. M.; Shi, Y. High-Rate Lithium-sulfur Batteries Promoted by Reduced Graphene Oxide Coating. *Chem. Commun.* **2012**, *48*, 4106−4108.
(18) Chen, S. R.; Zhai, Y. P.; Xu, G. L.; Jiang, Y. X.; Zhao, D. Y.; Li, J. T.; Huang, L.; Sun, S. G. Ordered Mesoporous Carbon/Sulfur Nanocomposite of High Performances as Cathode for Lithium-Sulfur Battery. *Electrochim. Acta* **2011**, *56*, 9549−9555.
(19) Liang, X. A.; Wen, Z. Y.; Liu, Y.; Zhang, H.; Huang, L. Z.; Jin, J. Highly Dispersed Sulfur in Ordered Mesoporous Carbon Sphere as a Composite Cathode for Rechargeable Polymer Li/S Battery. *J. Power Sources* **2011**, *196*, 3655−3658.
(20) Yuan, L. X.; Yuan, H. P.; Qiu, X. P.; Chen, L. Q.; Zhu, W. T. Improvement of Cycle Property of Sulfur-Coated Multi-walled Carbon Nanotubes Composite Cathode for Lithium/sulfur Batteries. *J. Power Sources* **2009**, *189*, 1141−1146.
(21) Han, S. C.; Song, M. S.; Lee, H.; Kim, H. S.; Ahn, H. J.; Lee, J. Y. Effect of Multiwalled Carbon Nanotubes on Electrochemical Properties of Lithium/Sulfur Rechargeable Batteries. *J. Electrochem. Soc.* **2003**, *150*, A889−A893.
(22) Chen, J. J.; Jia, X.; She, Q. J.; Wang, C.; Zhang, Q.; Zheng, M. S.; Dong, Q. F. The Preparation of Nano-Sulfur/MWCNTs and its Electrochemical Performance. *Electrochim. Acta* **2010**, *55*, 8062−8066.
(23) Chen, J. J.; Zhang, Q.; Shi, Y. N.; Qin, L. L.; Cao, Y.; Zheng, M. S.; Dong, Q. F. Hierarchical Architecture S/MWCNT Nanomicrosphere with Large Pores for Lithium Sulfur Battery. *Phys. Chem. Chem. Phys.* **2012**, *14*, 5376−5382.
(24) Guo, J. C.; Xu, Y. H.; Wang, C. S. Sulfur-Impregnated Disordered Carbon Nanotubes Cathode for Lithium Sulfur Batteries. *Nano Lett.* **2011**, *11*, 4288−4294.
(25) Yin, L. C.; Wang, J. L.; Yang, J.; Nuli, Y. N. A Novel Pyrolyzed Polyacrylonitrile-sulfur @ MWCNT Composite Cathode Material for High-rate Rechargeable Lithium/sulfur Batteries. *J. Mater. Chem.* **2011**, *21*, 6807−6810.
(26) Liang, X.; Wen, Z. Y.; Liu, Y.; Zhang, H.; Jin, J.; Wu, M. F.; Wu, X. W. A Composite of Sulfur and Polypyrrole-Multi Walled Carbon Combinatorial Nanotube as Cathode for Li/S Battery. *J. Power Sources* **2012**, *206*, 409−413.
(27) Xin, S.; Gu, L.; Zhao, N. H.; Yin, Y. X.; Zhou, L. J.; Guo, Y. G.; Wan, L. J. Smaller Sulfur Molecules Promise Better Lithium−Sulfur Batteries. *J. Am. Chem. Soc.* **2012**, *134*, 18510−18513.
(28) Dorfler, S.; Hagen, M.; Althues, H.; Tubke, J.; Kaskel, S.; Hoffmannd, M. J. High Capacity Vertical Aligned Carbon Nanotube/sulfur Composite Cathodes for Lithium-sulfur Batteries. *Chem. Commun.* **2012**, *48*, 4097−4099.

(29) Zhou, G. M.; Wang, D. W.; Li, F.; Hou, P. X.; Yin, L. C.; Liu, C.; Lu, G. Q.; Gentle, I. R.; Cheng, H. M. A Flexible Nanostructured Sulfur−Carbon Nanotube Cathode with High Rate Performance for Li-S Batteries. *Energy Environ. Sci.* **2012**, *5*, 8901−8906.
(30) Su, Y. S.; Fu, Y. Z.; Manthiram, A. Self-Weaving Sulfur-Carbon Composite Cathodes for High Rate Lithium-Sulfur Batteries. *Phys. Chem. Chem. Phys.* **2012**, *14*, 14495−14499.
(31) Ji, L. W.; Rao, M. M.; Zheng, H. M.; Zhang, L.; Li, Y. C.; Duan, W. H.; Guo, J. H.; Cairns, E. J.; Zhang, Y. G. Graphene Oxide as a Sulfur Immobilizer in High Performance Lithium/Sulfur Cells. *J. Am. Chem. Soc.* **2011**, *133*, 18520−18525.
(32) Liu, J.; Rinzler, A. G.; Dai, H. J.; Hafner, J. H.; Bradley, R. K.; Boul, P. J.; Lu, A.; Iverson, T.; Shelimov, K.; Huffman, C. B.; et al. Fullerene Pipes. *Science* **1998**, *280*, 1253−1256.
(33) Cooper, S. M.; Chuang, H. F.; Cinke, M. Gas Permeability of a Buckypaper Membrane. *Nano Lett.* **2003**, *3*, 189−192.
(34) Aurbach, D.; Pollak, E.; Elazari, R.; Salitra, G.; Kelley, C. S.; Affinito, J. On the Surface Chemical Aspects of Very High Energy Density Rechargeable Li−Sulfur Batteries and Energy Storage. *J. Electrochem. Soc.* **2009**, *156*, A694−A702.
(35) Yamin, H.; Penciner, J.; Corenshtain, A.; Elam, M.; Peled, E. The Electrochemical Behavior of Polysulfides in Tetrahydrofuran. *J. Power Sources* **1985**, *14*, 129−134.